

WMAP 5-year constraints on time variation of α and m_e in a detailed recombination scenario

Claudia G. Scóccola^{1,2*}, Susana. J. Landau^{3†}, Hector Vucetich¹,

¹ Facultad de Ciencias Astronómicas y Geofísicas. Universidad Nacional de La Plata,
Paseo del Bosque S/N 1900 La Plata, Argentina.

² Instituto de Astrofísica La Plata - CONICET

³ Departamento de Física, FCEyN, Universidad de Buenos Aires,
Ciudad Universitaria - Pab. 1, 1428 Buenos Aires, Argentina.

November 20, 2018

Abstract

We study the role of fundamental constants in an updated recombination scenario. We focus on the time variation of the fine structure constant α , and the electron mass m_e in the early Universe, and put bounds on these quantities by using data from CMB including WMAP 5-yr release and the 2dFGRS power spectrum. We analyze how the constraints are modified when changing the recombination scenario.

Time variation of fundamental constants is a prediction of theories that attempt to unify the four interactions in nature. Many efforts have been made to put observational and experimental constraints on such variations. Primordial light elements abundances produced at Big Bang nucleosynthesis (BBN) and cosmic microwave background radiation (CMB) are the most powerful tools to study the early universe and in particular, to put bounds

*fellow of CONICET

†member of the Carrera del Investigador Científico y Tecnológico CONICET

on possible variations of the fundamental constants between those early times and the present.

Previous analysis of CMB data (earlier than the WMAP five-year release) including a possible variation of α have been performed by refs. [1, 2, 3, 4] and including a possible variation of m_e have been performed by refs. [3, 4, 5]. In March 2008, WMAP team released data collected during the last five years [6]. Moreover, new processes relevant during the recombination epoch have been taken into account. Indeed, in the last years, helium recombination has been studied in great detail [7, 8, 9, 10], revealing the importance of these considerations on the calculation of the recombination history. Switzer & Hirata [8] presented a multi-level calculation for neutral helium recombination including, among other processes, the continuum opacity from H I photoionization. They found that at $z < 2200$ the increasing H I abundance begins to absorb photons out of the He I $2^1p \rightarrow 1^1s$ line, rapidly accelerating He I recombination, which finishes at $z \sim 1800$. Kholupenko et al [11] have considered the effect of the neutral hydrogen on helium recombination and proposed an approximated formula to take this effect into account. This has enabled its implementation on numerical codes such as RECFAST, since the complete calculations done by Switzer & Hirata take a large amount of computational time. Another improvement in the recombination scenario is the inclusion of the semi-forbidden transition $2^3p \rightarrow 1^1s$, the feedback from spectral distortions between $2^1p \rightarrow 1^1s$ and $2^3p \rightarrow 1^1s$ lines, and the radiative line transfer.

The release of new data from WMAP brings the possibility of updating the constraints on the time variation of fundamental constants. In this paper we study the variation of α and m_e in the improved recombination scenario. It could be argued that m_e is not a fundamental constant in the same sense as α is and that constraints on the Higgs vacuum expectation value ($\langle v \rangle$) are more relevant than bounds on m_e . However, in the recombination scenario the only consequence of the time variation of $\langle v \rangle$ is a variation in m_e .

The effect of a possible variation of α and/or m_e in the recombination scenario and in the CMB temperature and polarization spectra has been analyzed previously [12, 13, 14, 5]. Here we focus in the effect of the variation of α and m_e on the improved recombination scenario.

The recombination equations implemented in RECFAST in the detailed recombination scenario [15] including the fitting formulae of [11] are:

$$H(z)(1+z)\frac{dx_p}{dz} = (x_e x_p n_H \alpha_H - \beta_H (1 - x_p) e^{-h\nu_{H2s}/kT_M}) C_H, \quad (1)$$

$$\begin{aligned} H(z)(1+z)\frac{dx_{\text{HeII}}}{dz} = & (x_{\text{HeII}} x_e n_H \alpha_{\text{HeI}} - \beta_{\text{HeI}} (f_{\text{He}} - x_{\text{HeII}}) e^{-h\nu_{\text{HeI},2^1s}/kT_M}) C_{\text{HeI}} \\ & + \left(x_{\text{HeII}} x_e n_H \alpha_{\text{HeI}}^t - \frac{g_{\text{HeI},2^3s}}{g_{\text{HeI},1^1s}} \beta_{\text{HeI}}^t (f_{\text{He}} - x_{\text{HeII}}) e^{-h\nu_{\text{HeI},2^3s}/kT_M} \right) C_{\text{HeI}}^t, \end{aligned} \quad (2)$$

where

$$C_H = \frac{1 + K_H \Lambda_H n_H (1 - x_p)}{1 + K_H (\Lambda_H + \beta_H) n_H (1 - x_p)}, \quad (3)$$

$$C_{\text{HeI}} = \frac{1 + K_{\text{HeI}} \Lambda_{\text{He}} n_H (f_{\text{He}} - x_{\text{HeII}}) e^{h\nu_{ps}/kT_M}}{1 + K_{\text{HeI}} (\Lambda_{\text{He}} + \beta_{\text{HeI}}) n_H (f_{\text{He}} - x_{\text{HeII}}) e^{h\nu_{ps}/kT_M}}, \quad (4)$$

$$C_{\text{HeI}}^t = \frac{1}{1 + K_{\text{HeI}}^t \beta_{\text{HeI}}^t n_H (f_{\text{He}} - x_{\text{HeII}}) e^{h\nu_{ps}^t/kT_M}}. \quad (5)$$

The last term in eq. (2) accounts for the recombination through the triplets by including the semi-forbidden transition $2^3p \rightarrow 1^1s$. As remarked in [15], α_{HeI}^t is fitted with the same functional form used for the α_{HeI} singlets, with different values for the parameters, so the dependences on the fundamental constants are the same, being proportional to $\alpha^3 m_e^{-3/2}$. The two photon transition rates Λ_H and Λ_{He} depend on the fundamental constants as $\alpha^8 m_e$. The photoionization coefficients β are calculated as usual from the recombination coefficients α_c (with c standing for H, HeI and HeII), so their dependencies are known (see for example [4]).

The K_H , K_{HeI} and K_{HeI}^t quantities are the cosmological redshifting of the H Ly α , HeI 2^1p-1^1s and HeI 2^3p-1^1s transition line photons, respectively. In general, K and the Sobolev escape probability p_s are related through the following equations (taking HeI as an example):

$$K_{\text{HeI}} = \frac{g_{\text{HeI},1^1s}}{g_{\text{HeI},2^1p}} \frac{1}{n_{\text{HeI},1^1s} A_{2^1p-1^1s}^{\text{HeI}} p_s} \quad \text{and} \quad (6)$$

$$K_{\text{HeI}}^t = \frac{g_{\text{HeI},1^1s}}{g_{\text{HeI},2^3p}} \frac{1}{n_{\text{HeI},1^1s} A_{2^3p-1^1s}^{\text{HeI}} p_s}, \quad (7)$$

where $A_{\text{HeI}, 2^1\text{p}-1^1\text{s}}$ and $A_{\text{HeI}, 2^3\text{p}-1^1\text{s}}$ are the Einstein A coefficients of the He I $2^1\text{p}-1^1\text{s}$ and He I $2^3\text{p}-1^1\text{s}$ transitions, respectively. To include the effect of the continuum opacity due to H, based on the approximate formula suggested by ref. [11], p_{S} is replaced by the new escape probability $p_{\text{esc}} = p_{\text{S}} + p_{\text{con,H}}$ with

$$p_{\text{con,H}} = \frac{1}{1 + a_{\text{He}}\gamma^{b_{\text{He}}}}, \quad (8)$$

and

$$\gamma = \frac{\frac{g_{\text{HeI}, 1^1\text{s}}}{g_{\text{HeI}, 2^1\text{p}}} A_{2^1\text{p}-1^1\text{s}}^{\text{HeI}} (f_{\text{He}} - x_{\text{HeII}}) c^2}{8\pi^{3/2} \sigma_{\text{H}, 1\text{s}}(\nu_{\text{HeI}, 2^1\text{p}}) \nu_{\text{HeI}, 2^1\text{p}}^2 \Delta\nu_{\text{D}, 2^1\text{p}} (1 - x_{\text{p}})} \quad (9)$$

where $\sigma_{\text{H}, 1\text{s}}(\nu_{\text{HeI}, 2^1\text{p}})$ is the H ionization cross-section at frequency $\nu_{\text{HeI}, 2^1\text{p}}$ and $\Delta\nu_{\text{D}, 2^1\text{p}} = \nu_{\text{HeI}, 2^1\text{p}} \sqrt{2k_{\text{B}}T_{\text{M}}/m_{\text{He}}c^2}$ is the thermal width of the He I $2^1\text{p}-1^1\text{s}$ line. The cross-section for photo-ionization from level n is [16]:

$$\sigma_n(Z, h\nu) = \frac{2^6 \alpha \pi a_0^2}{3\sqrt{3}} \frac{n}{Z^2} (1 + n^2 \epsilon)^{-3} g_{II}(n, \epsilon) \quad (10)$$

where $g_{II}(n, \epsilon) \simeq 1$ is the Gaunt-Kramers factor, and $a_0 = \hbar/(m_e c \alpha)$ is the Bohr radius, so $\sigma_{\text{H}, 1\text{s}}(\nu_{\text{HeI}, 2^1\text{p}})$ is proportional to $\alpha^{-1} m_e^{-2}$.

The transition probability rates $A_{\text{HeI}, 2^1\text{p}-1^1\text{s}}$ and $A_{\text{HeI}, 2^3\text{p}-1^1\text{s}}$ can be expressed as follows [17]:

$$A_{i-j}^{\text{HeI}} = \frac{4\alpha}{3c^2} \omega_{ij}^3 |\langle \psi_i | r_1 + r_2 | \psi_j \rangle|^2 \quad (11)$$

where ω_{ij} is the frequency of the transition, and $i(j)$ refers to the initial (final) state of the atom. First we will analyze the dependence of the bra-ket. To first order in perturbation theory, all wavefunctions can be approximated to the respective wavefunction of hydrogen. Those can be usually expressed as $\exp(-qr/a_0)$ where a_0 is the Bohr radius and q is a number. It can be shown that any integral of the type of Eq. (11) can be solved with a change of variable $x = r/a_0$. If the wave functions are properly normalized, the dependence on the fundamental constants comes from the operator, namely $r_1 + r_2$. Thus, the dependence of the bra-ket goes as a_0 . On the other hand, ω_{ij} is proportional to the difference of energy levels and thus its dependence on the fundamental constants is $\omega_{ij} \simeq m_e \alpha^2$. Consequently, the dependence of the transition probabilities of HeI on α and m_e is

$$A_{i-j}^{\text{HeI}} \simeq m_e \alpha^5 \quad (12)$$

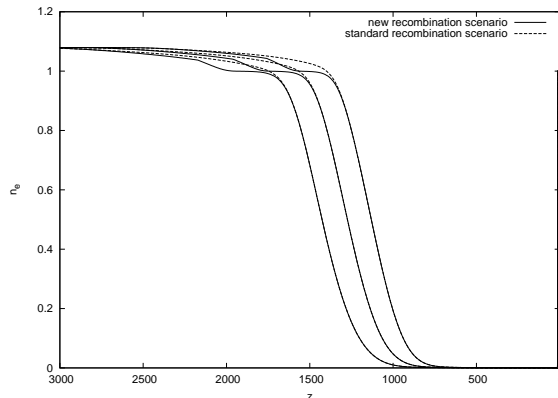


Figure 1: Ionization history allowing α to vary with time. From left to right, the values of $\frac{\alpha}{\alpha_0}$ are 1.05, 1.00, and 0.95, respectively. The dotted lines correspond to the standard recombination scenario, and the solid lines correspond to the updated one.

In Fig. 1 we show how a variation in the value of α at recombination affects the ionization history, moving the redshift at which recombination occurs to earlier times for larger values of α . The difference between the functions when the two different recombination scenarios are considered, for a given value of α , is smaller than the difference that arise when varying the value of α . Something similar happens when varying m_e .

With regards to the fitting parameters a_{He} and b_{He} , since detailed calculation of their values are not available yet, it is not possible to determine the effect that a variation of α or m_e would have on these new parameters. Wong et al [15] have shown that they must be known at the 1% level for future Planck data. In this letter, however, we are dealing with the 5 yr data from WMAP satellite and this accuracy is not required. To come to this conclusion, we have calculated the temperature, polarization and cross correlation CMB spectra, allowing the parameters a_{He} and b_{He} to vary at the 50% level. We found that for the temperature and polarization spectra, the variation is always lower than the observational error (1% for temperature and almost 40 % in polarization). The largest variations occur in the cross

correlation CMB spectra (C_ℓ^{TE}). In this case, we have calculated the observational errors divided by the value of the C_ℓ 's of all measured C_ℓ^{TE} and compared them with the relative variation in the C_ℓ 's induced when changing a_{He} and b_{He} by a 50%. In all of the cases the first quantity is several orders of magnitude greater than the variation of the C_ℓ 's. Therefore, in order to analyze WMAP5 data, there is no need to modify these parameters.

To put constraints on the variation of α and m_e during recombination time in the detailed recombination scenario studied here, we introduced the dependencies on the fundamental constants explicitly in the latest version of RECFAST code [18], which solves the recombination equations. We performed our statistical analysis by exploring the parameter space with Monte Carlo Markov chains generated with the publicly available CosmoMC code of ref. [19] which uses the Boltzmann code CAMB [20] and RECFAST to compute the CMB power spectra. We modified them in order to include the possible variation of α and m_e at recombination. We ran eight Markov chains and followed the convergence criterion of ref. [21] to stop them when $R - 1 < 0.0180$. Results are shown in Table 1 and Figure 2.

The observational set used for the analysis was data from the WMAP 5-year temperature and temperature-polarization power spectrum [6], and other CMB experiments such as CBI [22], ACBAR [23], and BOOMERANG [24, 25], and the power spectrum of the 2dFGRS [26]. We have considered a spatially-flat cosmological model with adiabatic density fluctuations, and the following parameters:

$$P = \left(\Omega_B h^2, \Omega_{CDM} h^2, \Theta, \tau, \frac{\Delta\alpha}{\alpha_0}, \frac{\Delta m_e}{(m_e)_0}, n_s, A_s \right), \quad (13)$$

where $\Omega_{CDM} h^2$ is the dark matter density in units of the critical density, Θ gives the ratio of the comoving sound horizon at decoupling to the angular diameter distance to the surface of last scattering, τ is the reionization optical depth, n_s the scalar spectral index and A_s is the amplitude of the density fluctuations.

In Fig. 2 we show the marginalized posterior distributions for the cosmological parameters, $\Delta\alpha/\alpha_0$, and $\Delta m_e/(m_e)_0$, which are the variation in the values of those fundamental constants between recombination epoch and the present. The three successively larger two dimensional contours in each panel correspond to the 68%-, 95%-, and 99%- probability levels, respectively. In the diagonal, the one dimensional likelihoods show the posterior distribution of the parameters.

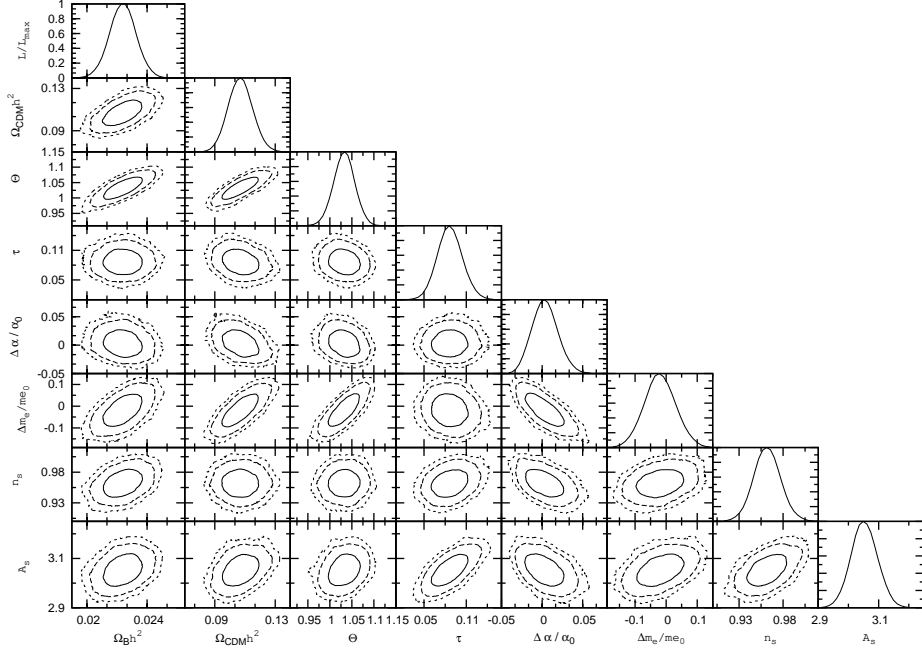


Figure 2: Marginalized posterior distributions obtained with CMB data, including the WMAP 5-year data release plus 2dFGRS power spectrum. The diagonal shows the posterior distributions for individual parameters, the other panels shows the 2D contours for pairs of parameters, marginalizing over the others.

In Table 1 we show the results of our statistical analysis, and compare them with the ones we have presented in ref. [4], which were obtained in the standard recombination scenario (i.e. the one described in [27], which we denote PS), and using WMAP3 [28, 29] data. The constraints are tighter in the current analysis, which is an expectable fact since we are working with more accurate data from WMAP. The bounds obtained are consistent with null variation, for both α and m_e , but in the present analysis, the 68% confidence limits on the variation of both constants have changed. In the case of α , the present limit is more consistent with null variation than the previous one, while in the case of m_e the single parameters limits have moved toward lower values. To study the origin of this difference, we perform another statistical analysis, namely the analysis of the standard recombination

parameter	wmap5 + NS	wmap5 + PS	wmap3 + PS
$\Omega_b h^2$	$0.02241^{+0.00084}_{-0.00084}$	$0.02242^{+0.00086}_{-0.00085}$	$0.0218^{+0.0010}_{-0.0010}$
$\Omega_{CDM} h^2$	$0.1070^{+0.0078}_{-0.0078}$	$0.1071^{+0.0080}_{-0.0080}$	$0.106^{+0.011}_{-0.011}$
Θ	$1.033^{+0.023}_{-0.023}$	$1.03261^{+0.024}_{-0.023}$	$1.033^{+0.028}_{-0.029}$
τ	$0.0870^{+0.0073}_{-0.0081}$	$0.0863^{+0.0077}_{-0.0084}$	$0.090^{+0.014}_{-0.014}$
$\Delta\alpha/\alpha_0$	$0.004^{+0.015}_{-0.015}$	$0.003^{+0.015}_{-0.015}$	$-0.023^{+0.025}_{-0.025}$
$\Delta m_e/(m_e)_0$	$-0.0193^{+0.049}_{-0.049}$	$-0.017^{+0.051}_{-0.051}$	$0.036^{+0.078}_{-0.078}$
n_s	$0.962^{+0.014}_{-0.014}$	$0.963^{+0.015}_{-0.015}$	$0.970^{+0.019}_{-0.019}$
A_s	$3.053^{+0.042}_{-0.041}$	$3.05203^{+0.04269}_{-0.04257}$	$3.054^{+0.073}_{-0.073}$
H_0	$70.3^{+5.9}_{-5.8}$	$70.3^{+6.1}_{-6.0}$	$70.4^{+6.6}_{-6.8}$

Table 1: Mean values and 1σ errors for the parameters including α and m_e variations. NS stands for the new recombination scenario, and PS stands for the previous one.

scenario (PS) together with WMAP5 data and the other CMB data sets and the 2dFGRS power spectrum. The results are also shown in Table 1. We see that the changes in the results are due to the new WMAP data set, and not to the new recombination scenario. In Fig. 3 we compare the probability distribution for $\Delta\alpha/\alpha_0$ and also for $\Delta m_e/(m_e)_0$, in different scenarios and with different data sets.

In Fig. 4 we compare the 95%- probability contour level for the parameters, and their one dimensional distributions, for two different analysis in the standard recombination scenario, namely the one with WMAP5 data (dashed lines) and the one with WMAP3 data (solid lines). The contours are smaller in the former case, which is expectable since that data set is more accurate. For the fundamental constants, the contours notably shrink. Moreover, the constraints are shifted to a region of the parameter space closer to that of null variation in the case of α . On the other hand, limits on the variation of m_e are shifted to negative values, but still consistent with null variation. From the one dimensional likelihoods we see that the the peak of the likelihood has moved for $\Omega_b h^2$. The obtained results for the cosmological parameters are

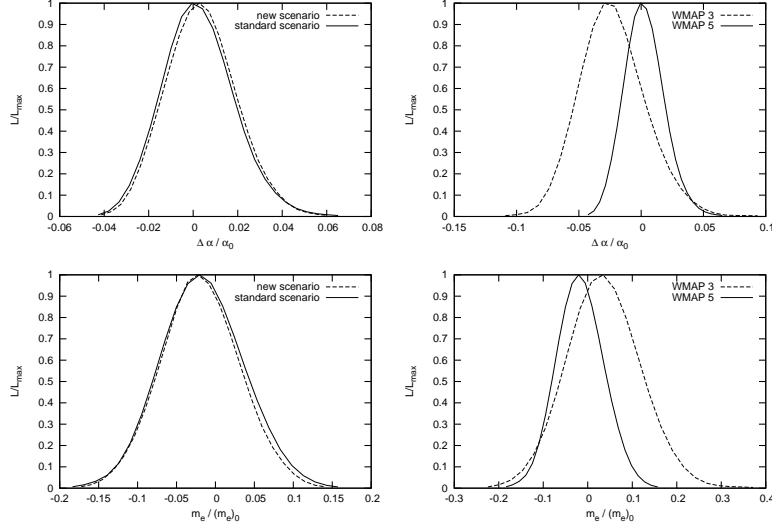


Figure 3: One dimensional likelihood for $\frac{\Delta\alpha}{\alpha_0}$ (upper row) and $\frac{\Delta m_e}{(m_e)_0}$ (lower row). Left: for WMAP5 data and two different recombination scenarios. Right: comparison for the standard recombination scenario, between the WMAP3 and WMAP5 data sets.

in agreement within 1σ with the ones obtained by the WMAP collaboration [30], without considering variation of fundamental constants.

References

- [1] Martins, C. J., Melchiorri, A., Trotta, R., Bean, R., Rocha, G., Avelino, P. P., & Viana, P. T. 2002, Phys.Rev. D66, 023505
- [2] Rocha, G., Trotta, R., Martins, C. J. A. P., Melchiorri, A., Avelino, P. P., & Viana, P. T. P. 2003, New Astronomy Review, 47, 863
- [3] Ichikawa, K., Kanzaki, T., & Kawasaki, M. 2006, Phys.Rev. D74, 023515
- [4] Landau, S.J., Mosquera, M.E., Scóccola, C. and Vucetich, H. Accepted in Phys.Rev. D (2008)
- [5] Yoo, J. J., & Scherrer, R. J. 2003, Phys.Rev. D67, 043517

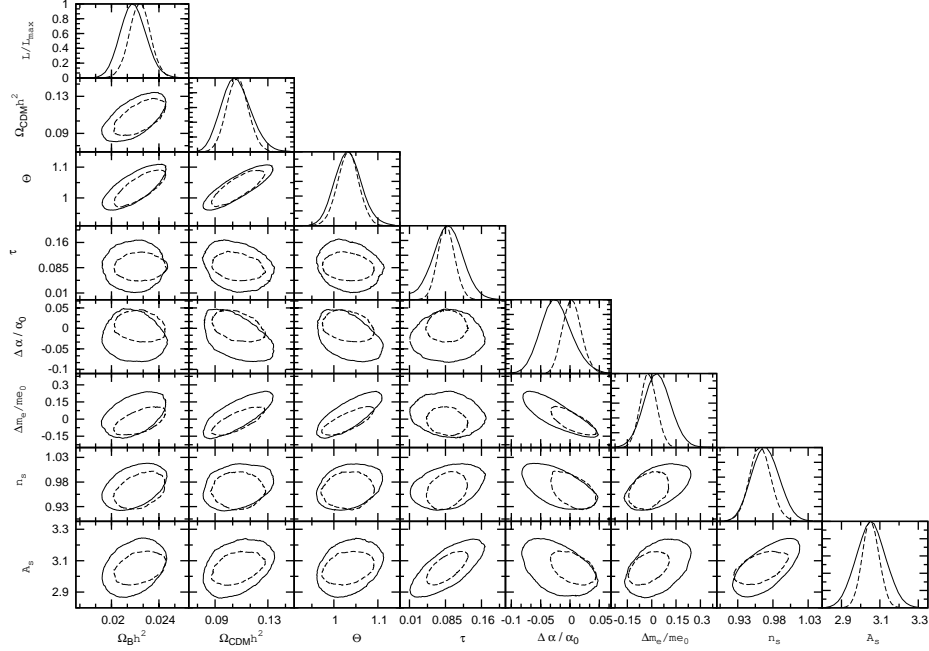


Figure 4: Comparison between the 95%- confidence levels of WMAP3 (solid line) with those of WMAP5 (dashed line). In the diagonal, we compare the one dimensional likelihoods in these two cases.

- [6] Nolita, M. R., et al. 2008, ArXiv e-prints, 803, arXiv:0803.0593
- [7] Dubrovich, V. K., & Grachev, S. I. 2005, Astronomy Letters, 31, 359
- [8] Switzer, E. R., & Hirata, C. M. 2008, Phys.Rev. D77, 083006
- [9] Hirata, C. M., & Switzer, E. R. 2008, Phys.Rev. D77, 083007
- [10] Switzer, E. R., & Hirata, C. M. 2008, Phys.Rev. D77, 083008
- [11] Kholupenko, E. E., Ivanchik, A. V., & Varshalovich, D. A. 2007, Mon.Not.Roy.Astron.Soc. 378, L39
- [12] Kaplinghat, M., Scherrer, R. J., & Turner, M. S. 1999, Phys.Rev. D60, 023516

- [13] Hannestad, S. 1999, Phys.Rev. D60, 023515
- [14] Kujat, J., & Scherrer, R. J. 2000, Phys.Rev. D62, 023510
- [15] Wong, W. Y., Moss, A., & Scott, D. 2008, Mon.Not.Roy.Astron.Soc. 386, 1023
- [16] Seaton, M. J. 1959, Mon.Not.Roy.Astron.Soc. 119, 81
- [17] Drake, G. W. F., & Morton, D. C. 2007, Astrophys.J.Suppl.Ser. 170, 251
- [18] Seager, S., Sasselov, D. D., & Scott, D. 1999, Astrophys.J.Letters 523, L1
- [19] Lewis, A., & Bridle, S. 2002, Phys.Rev. D66, 103511
- [20] Lewis, A., Challinor, A., & Lasenby, A. 2000, Astrophys.J.538, 473
- [21] Raftery, A.E. & Lewis, S.M. (1992) In Bayesian Statistics, (Bernaro, J.M.,ed), p.765. OUP.
- [22] Readhead, A. C. S., et al. 2004, Astrophys.J.609, 498
- [23] Kuo, C. L., et al. 2004, Astrophys.J.600, 32
- [24] Piacentini, F., et al. 2006, Astrophys.J.647, 833
- [25] Jones, W. C., et al. 2006, Astrophys.J.647, 823
- [26] Cole, S., et al. 2005, Mon.Not.Roy.Astron.Soc. 362, 505
- [27] Seager, S., Sasselov, D. D., & Scott, D. 2000, Astrophys.J.Supp.Ser. 128, 407
- [28] Hinshaw, G., et al. 2007, Astrophys.J.Supp.Ser. 170, 288
- [29] Page, L., et al. 2007, Astrophys.J.Supp.Ser. 170, 335
- [30] Dunkley, J., et al. 2008, ArXiv e-prints, 803, arXiv:0803.0586